

Constraining the Inclination of the Low Mass X-ray Binary Cen X-4

E. Hammerstein & E. Cackett

*Department of Physics & Astronomy
Wayne State University*

Abstract

We present the results of ellipsoidal light curve modeling of the low mass X-ray binary (LMXB) Cen X-4 in order to constrain the inclination of the system and mass of the neutron star. The light curve was obtained in May 2008 over a period of three nights at Magellan. After calibrations, we were able to obtain apparent magnitudes for the system using differential photometry. We used an ellipsoidal modeling code to fit the light curve and the results of the modeling yield an inclination of $32.0^\circ \pm 0.8^\circ$, which is consistent with previous calculations of the system's inclination but with much improved uncertainties. When combined with the mass function, this inclination yields a neutron star mass of $1.93 \pm 0.13 M_\odot$, which is also consistent with previous estimates of the mass of the compact object in Cen X-4. We discuss the implications of assumptions made during the modeling process as well as numerous free parameters and their effects on the resulting inclination.

1 Introduction

1.1 Neutron Stars & the Equation of State for Dense Matter

Neutron stars are a unique and important setting for studying dense matter as they contain the densest naturally occurring observable matter in the universe. Studying neutron stars can help in setting constraints on the equation of state (EOS) for this dense neutron matter, which has yet to be well defined. The EOS, which is a relation between the pressure and the density, can be explored and constrained through the mass-radius relation. Current data on neutron star masses and radii suggest that the EOS near the nuclear saturation density is soft, which means that the pressure there is low, while the existence of higher mass neutron stars suggests that the EOS stiffens at higher densities (Lattimer & Prakash, 2016). Although observations of neutron stars have already been performed, mass and radii measurements for these types of stars still need to be more tightly constrained to obtain a more accurate lower limit for the maximum mass of a neutron star and constrain the high density end of the EOS.

1.2 Light Curves of Low Mass X-ray Binary Systems

LMXBs are a type of binary system in which a compact object, a neutron star or black hole, is accompanied by a secondary star of lower mass. If the secondary star in a LMXB fills its Roche-lobe, it may accrete matter onto the compact object. Since these are binary systems it is possible to measure the mass of the compact object by observing orbital variability. In order to measure the mass one needs to know the inclination of the system.

Once determined, the inclination of the binary system can then be used to calculate the mass function of the system, or if the value of the mass function is known can be used to find the mass of the neutron star, using the following equation:

$$f(M) = \frac{P_{orb}K_2^3}{2\pi G} = \frac{M_1 \sin^3 i}{(1+q)^2} \quad (1)$$

where P_{orb} is the orbital period in days, K_2 is the peak radial velocity of the secondary star, M_1 is the mass of the compact object, i is the inclination, and q is the mass ratio. It is easily seen that tighter constraints on the inclination can be used to constrain the mass M_1 .

The geometry of these types of systems at certain points in their orbital period allows for ellipsoidal variations in their light curves. Since the secondary star fills its Roche-lobe it is no longer spherical and appears more “tear-drop”-like in shape. At a certain time in their orbital period, the secondary star and its filled Roche-lobe may be fully visible and the system will appear brighter than at a different point where the filled Roche-lobe is not seen as it is either positioned in front of the secondary or is blocked by the secondary itself. At these points the light curve will appear dimmer. These ellipsoidal variations in the light curve will be highly dependent on the inclination of the system as there will be either more or less obscuration of the Roche-lobe depending on the angle.

1.3 The LMXB Cen X-4

Cen X-4 is an LMXB in which the compact object is a neutron star and the secondary is approximately a K4 V type star with $T_{eff}=4500$ K and $\log g=3.9$ (González Hernández et al., 2005). It was discovered in 1969 by the Vela 5B satellite during one of its X-ray outbursts (Conner et al., 1969). This system is one of the closest LMXBs to Earth, allowing for highly accurate photometric measurements and spectral analysis.

Cen X-4 has been a well studied system since its discovery, however, mass measurements for the neutron star have not been well constrained. The compact object was classified by Mat-suoka et al. (1980) as a neutron star due to the observation of a Type I X-ray burst. Shahbaz et al. (2014) determined $K_2=147.3\pm 0.3\text{kms}^{-1}$, $P_{orb}=0.629059\pm 0.000017\text{d}$, $\gamma=194.5\pm 0.2\text{kms}^{-1}$, and $T_0=\text{HJD}2454626.6214\pm 0.0002$, which are used in the calculations and modeling in this paper, along with the mass function, $f(M)$, equal to $0.201\pm 0.004 M_\odot$ obtained by D’Avanzo et al. (2005). Shahbaz et al. (2014) also determined q to be 0.1755 ± 0.0025 and i to be $32^\circ_{-2}^{+8}$.

Previous papers have used several different methods to determine the system’s inclination and mass ratio. The first attempt at constraining the system’s inclination angle was made by Shahbaz et al. (1993) by fitting the quiescent light curve with an ellipsoidal model, which assumed no contamination from the accretion disk, and was determined to be in the range of $31^\circ\text{--}54^\circ$. Khargharia et al. (2010) revised this estimate by determining the contribution of the secondary star in the infrared to remodel the original Shahbaz et al. (1993) light curves, and determined i to be $35^\circ_{-1}^{+4}$. Casares et al. (2007) compared the observed spectrum of the secondary star with a template star combined with a limb-darkened rotation profile to find q . Most recently, Shahbaz et al. (2014) determined i and q by using an X-ray binary model to model the shape of the secondary star’s Roche-lobe distorted absorption line profiles. In this paper, we determine the inclination angle of the Cen X-4 system by modeling the ellipsoidal variations in the system’s infrared light curve and thus measure the mass of the neutron star.

Filter	Exposures
J	19
H	20
K	113

Table 1: The number of useful exposures for each filter is shown.

Object	RA	Dec
Cen X-4	14:58:21.879	-31:40:6.36
Star 1	14:58:21.655	-31:39:47.43
Star 2	14:58:20.247	-31:39:38.29
Star 3	14:58:23.164	-31:39:51.05

Table 2: The RA and Dec of each of the source used in the relative photometry process. The reference stars were chosen for their non-variability and brightness as compared to Cen X-4.

2 Observations & Data Reduction

2.1 Observations with Magellan

We obtained photometry of Cen X-4 using the 6.5-m Magellan telescope at Las Campanas Observatory, over three nights during May 2008. The Persson’s Auxiliary Nasmyth Infrared Camera (PANIC) was used to observe Cen X-4 in the J, H, and K bandpass filters, covering 1 – 2.5 microns (Martini et al., 2004). The infrared is best for observing the ellipsoidal variability of X-ray binaries, as there is less contamination from the accretion disk at these wavelengths as opposed to visual wavelengths (Shahbaz et al., 1993). The typical exposure time with PANIC was 10 seconds taken in a dice-5 pattern. The number of useful exposures for each filter is seen in Table 1.

2.2 Data Reduction & Photometry

We performed calibrations of the images taken, which included dark frame corrections and flat-fielding using twilight flats. Bias subtraction is unnecessary when using PANIC. To obtain the source flux, we used aperture photometry to acquire source counts and then relative photometry to acquire relative fluxes for Cen X-4 and the reference stars. Table 2 lists the right ascension and declination of each source, including Cen X-4 and the three reference stars used for the relative photometry and Figure 1 shows the reference stars and Cen X-4 in a single exposure. The relative fluxes of each source were then converted to apparent magnitudes using magnitudes from the 2MASS survey. Photometric errors were calculated using both statistical errors from the aperture photometry and the standard deviation of the reference stars over all images added in quadrature. In order to account for the highest possible error we chose the reference star with the highest variability, star 1, whose relative standard deviation (RSD) is 1.17%, to calculate errors. Stars 2 and 3 have RSDs of 0.49% and 0.89%, respectively. Figure 2 shows the reference stars in relation to Cen X-4 in the K band. We performed phase folding of the light curves in order to obtain a single period for the binary system, using an orbital period of 0.629059 ± 0.000017 d and $T_0 = \text{HJD } 2454626.6214 \pm 0.0002$ from Shahbaz et al. (2014) to perform the phase folding. After the single phase light curve was obtained we performed ellipsoidal modeling of the light curve, which is discussed in the next section.

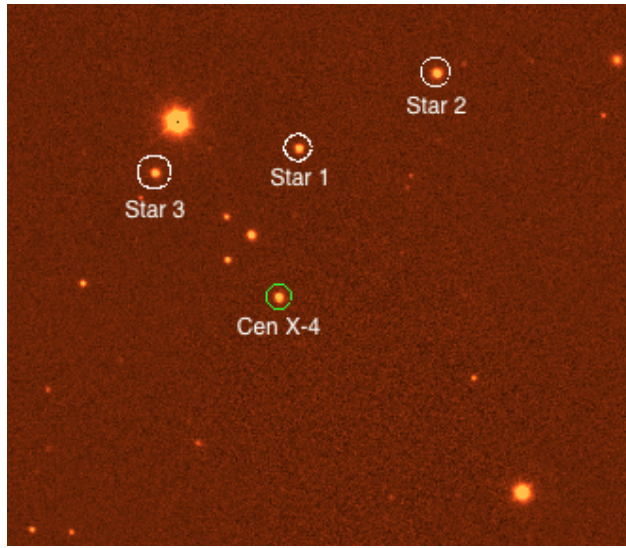


Figure 1: The three reference stars along with Cen X-4 are circled and labeled.

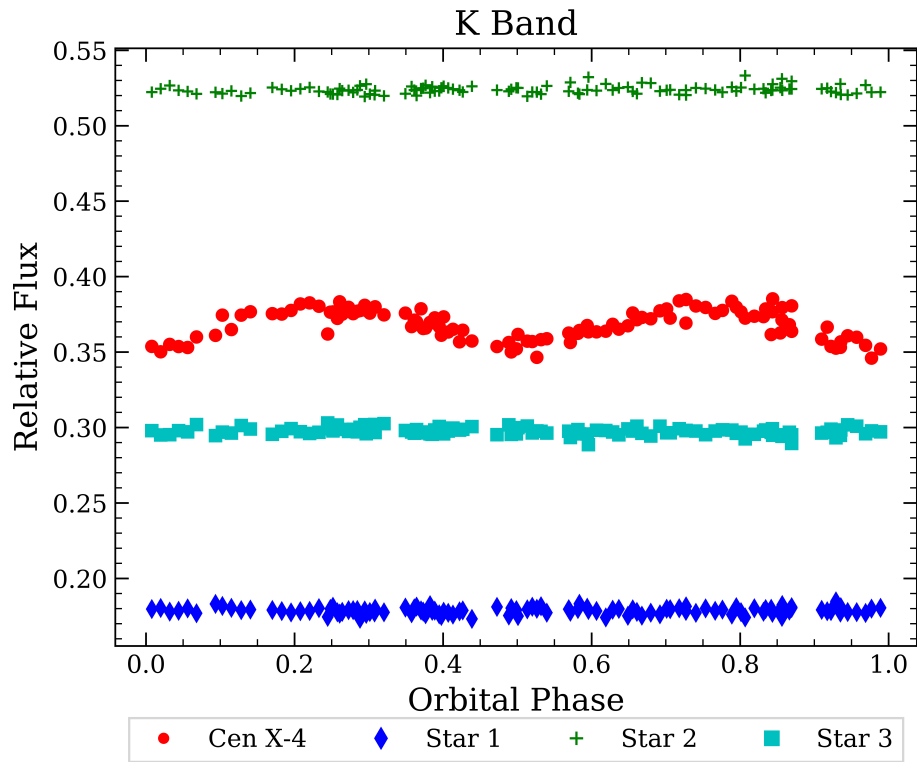


Figure 2: The relative flux light curve of the three reference stars and Cen X-4 in the K band.

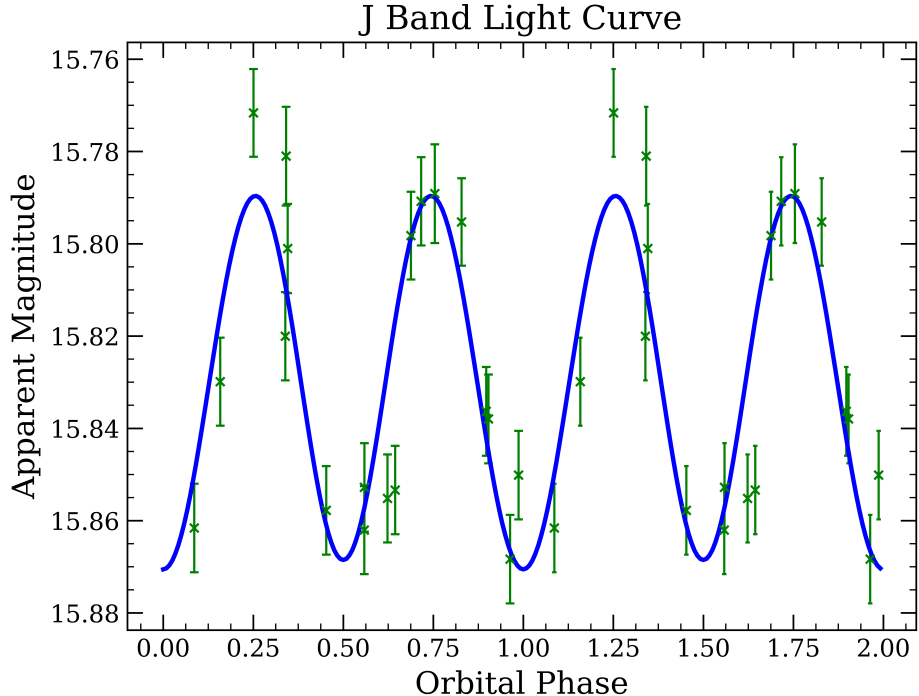


Figure 3: The phase folded J band light curve. The model is shown here as a blue line and green light curve points have been repeated over a second phase for clarity.

3 Light Curves and Modeling Results

3.1 The Phase Folded Light Curves

We present the phase folded light curves of Cen X-4 in the J, H, and K bands in Figures 3, 4, and 5. Errors on the photometry were calculated using error propagation when converting the source counts to apparent magnitudes. The model is also present on the light curves, which is discussed in more detail in the next section.

3.2 Modeling Results

We employed the use of the Eclipsing Light Curve (ELC) code written by Orosz & Hauschildt (2000) in order to fit a model to the shape of the Cen X-4 light curve and obtain an inclination based on the best fit model produced by the optimizer code. We began by exploring the parameters of the system, namely the mass ratio, effective temperature of the secondary star, accretion disk radius, and accretion disk temperature. Additionally, we created models with and without an accretion disk while varying only the inclination or by varying the inclination in addition to the effective temperature of the secondary star or the mass ratio. Fixed parameters included P_{orb} , K_2 , $f(M)$, and γ , whose values are taken from Shahbaz et al. (2014) and D’Avanzo et al. (2005). All other parameters of the model were set to the default. We set i to vary in the range of $20^\circ < i < 50^\circ$. In cases where disk parameters are fixed, the default values for T_{disk} and R_{disk} are 30000 K and 0.75, respectively. Table 3 shows the results of these models and the values corresponding to any additional free parameters.

From Table 3, our best fit model is model 1, which yields an inclination of $32.0^\circ \pm 0.8^\circ$. This model varies both the inclination and the effective temperature of the secondary star, which is

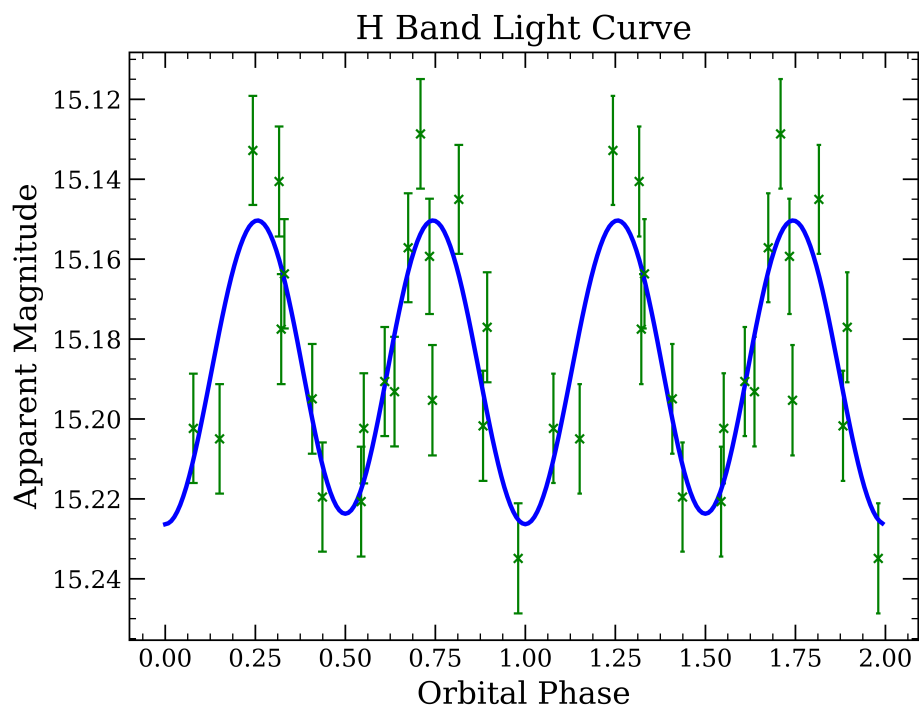


Figure 4: The phase folded H band light curve. The model is shown here as a blue line and the green light curve points have been repeated over a second phase for clarity.

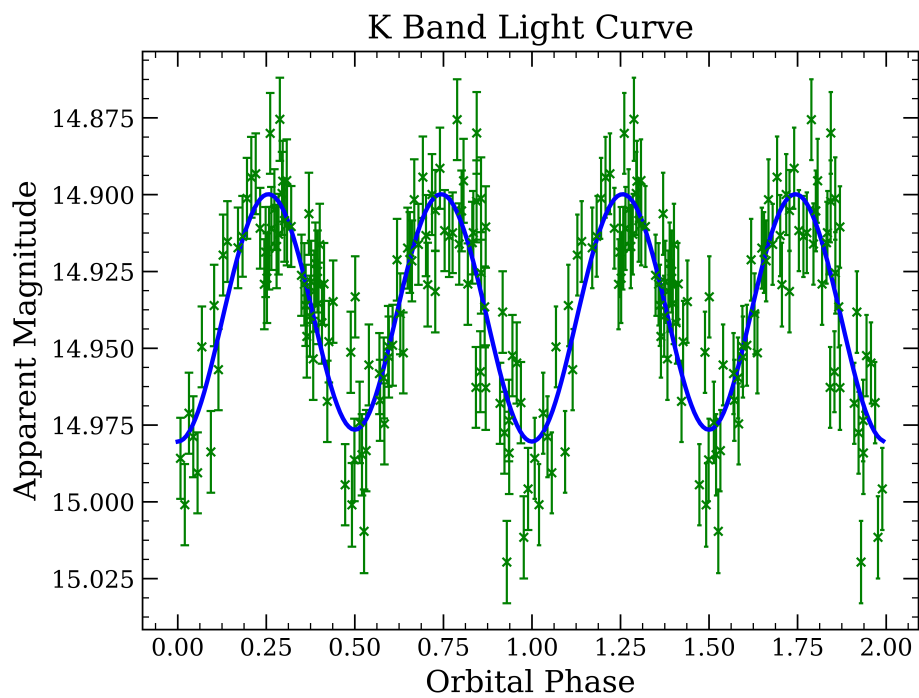


Figure 5: The phase folded K band light curve. The model is shown here as a blue line and the green light curve points have been repeated over a second phase for clarity.

Model	Free Parameters	Notes	χ^2_{min}	Parameter Values		$M_{NS} (M_{\odot})$
1	i, T_{eff}	No disk	286.3	$32.0^{\circ} \pm 0.8^{\circ}$	3033 ± 37 K	1.93 ± 0.13
2	i, q	No disk	289.8	$32.2^{\circ+1.2^{\circ}}_{-0.7^{\circ}}$	10 ± 4.9	$1.91^{+0.18}_{-0.12}$
3	i, T_{disk}	With disk	290.5	$33.0^{\circ+3.0^{\circ}}_{-0.7^{\circ}}$	2005^{+32753}_{-5} K	$1.78^{+0.42}_{-0.1}$
4	i	With disk	291.0	$35.1^{\circ+0.8^{\circ}}_{-0.7^{\circ}}$	–	1.52 ± 0.1
5	i, R_{disk}	With disk	290.2	$33.5^{\circ+1.9^{\circ}}_{-1.2^{\circ}}$	$0.04^{+0.96}_{-0.04}$	$1.71^{+0.25}_{-0.15}$
6	i, T_{eff}	With disk	288.1	$37.1^{\circ+1.0^{\circ}}_{-1.8^{\circ}}$	3054.8^{+4470}_{-46} K	$1.32^{+0.1}_{-0.15}$
7	i, q	With disk	290.7	$35.2^{\circ} \pm 0.7^{\circ}$	9.9 ± 5.7	1.45 ± 0.1
8	i	No disk	290.5	$33.0^{\circ} \pm 0.7^{\circ}$	–	1.78 ± 0.1

Table 3: Each model that we created is listed here along with the free parameters, minimum χ^2 , value of the inclination, and value of any other free parameter included in the model. Here, i is the inclination, T_{eff} is the effective temperature of the secondary star, q is the mass ratio (defined in the ELC code as the ratio of the neutron star to the secondary), and R_{disk} and T_{disk} are the outer radius and temperature of the accretion disk, respectively. M_{NS} is the calculated mass of the neutron star based on the parameters of the model. Each model as 150 degrees of freedom, other than models 4 and 8 which have 151 degrees of freedom.

found to be 3033 ± 37 K. The accretion disk is not taken into account and we set T_{eff} to vary in the range of 2000–8000 K, which well encompasses the estimated effective temperature for the secondary star based on spectral type. The model has a $\chi^2_{\nu, min}$ of 1.91 and the χ^2 distribution for the parameters of this model can be seen in Figure 6.

We combined the inclination obtained from the model with the value of the mass function (Equation 1) using values of P_{orb} , K_2 , and q calculated by Shahbaz et al. (2014) to obtain a neutron star mass of $1.93 \pm 0.13 M_{\odot}$, which is consistent with previous estimates of the mass.

4 Discussion

4.1 Effects of Model Assumptions

We modeled the light curves in several different ways in order to better understand the parameter space and implications of assumptions made during the modeling process. Model 1 finds the best fit for the light curve at $i = 32.0^{\circ} \pm 0.8^{\circ}$ and an effective temperature of 3033 ± 37.3 K for the secondary star. While this effective temperature is still within the range of estimated effective temperatures for the secondary star, a well accepted estimate for T_{eff} is 4500 K (González Hernández et al., 2005). When considering the results presented by Shahbaz et al. (2014), who used $T_{eff} = 4500$ K in their modeling, there is no substantial difference between our inclination measurement and the measurement presented by Shahbaz et al. (2014), despite the differences in effective temperature used in the model. Khargharia et al. (2010) noted that varying T_{eff} between 3700 K and 4500 K only changes the inclination by $\sim 1^{\circ}$. In our models 1 and 6, the optimized effective temperatures are similar but the inclinations have a difference of $\sim 5^{\circ}$. The accretion disk is accounted for in model 6. This implies that the effective temperature may not have a large effect on the outcome of the model, but that assumptions about the accretion disk do. This is further illustrated in the differences between models 4 and 8, which only vary the inclination either with or without the accretion disk but have a difference of $\sim 2^{\circ}$.

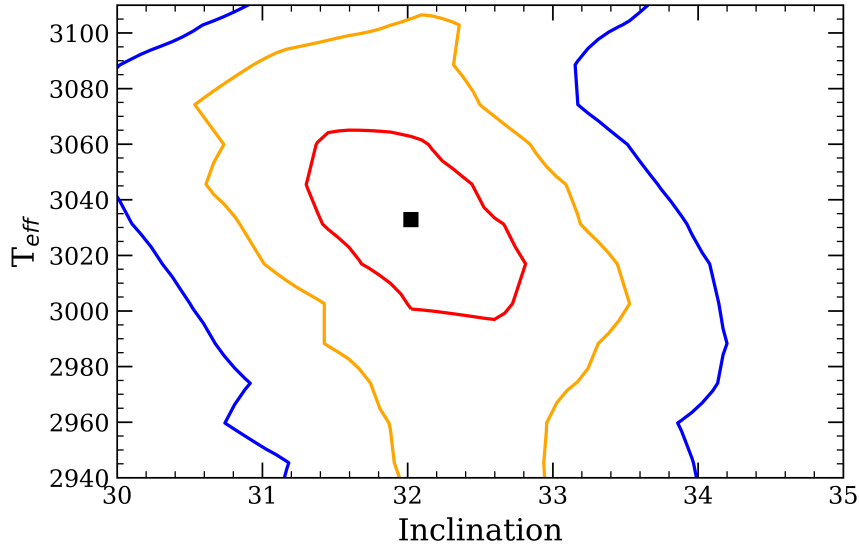


Figure 6: Here we see the χ^2 distribution for model 1. The 1, 2 and 3σ contours are shown. The square marker indicates the combination of parameters with the lowest χ^2 .

The value of the inclination is most greatly affected by whether or not there is an accretion disk present in the model in cases where the accretion disk parameters are held fixed (models 4, 6, and 7). The models that vary accretion disk parameters (T_{disk} and R_{disk}), do not find substantially different values of the system inclination. This is perhaps because the model finds a best fit at extremely low values for T_{disk} and R_{disk} , making the accretion disk almost non-existent in those cases. Without taking an accretion disk into account, we find an inclination consistent with previous estimates obtained through other methods of measuring the inclination. Khargharia et al. (2010) remodeled the original Shahbaz et al. (1993) light curves, accounting for contamination from the disk. This yielded an inclination of $35^{\circ+4}_{-1}$, with which our models 4, 6 and 7 in Table 3 are more consistent. Shahbaz et al. (2014) noted that their model, which produced an inclination of $32^{\circ+8}_{-2}$ (with which our determined inclination agrees), does not rely on assumptions about contamination from the accretion disk. While our model agrees with both of these estimates, it is seen from Table 3 that models that do not account for contamination from the accretion disk have typically better fits to the light curve but consistently lower inclinations than the models accounting for the disk.

5 Conclusions

We obtained photometry of the LMXB Cen X-4 and have accurately determined the system parameters i and hence M_{NS} to be $32.0^{\circ} \pm 0.8^{\circ}$ and $1.93 \pm 0.13 M_{\odot}$, respectively. Our values for inclination and M_{NS} are consistent with other estimates of the system parameters found through different methods. Although our measurements do not account for contamination from the accretion disk, our values are consistent with previous estimates that do not depend on assumptions about contribution from the disk.

References

- Casares, J., Bonifacio, P., González Hernández, J. I., Molaro, P., & Zoccali, M. 2007, *A&A*, 470, 1033
- Conner, J. P., Evans, W. D., & Belian, R. D. 1969, *ApJ*, 157, L157
- D'Avanzo, P., Campana, S., Casares, J., Israel, G. L., Covino, S., Charles, P. A., & Stella, L. 2005, *A&A*, 444, 905
- González Hernández, J. I., Rebolo, R., Israelian, G., Casares, J., Maeda, K., Bonifacio, P., & Molaro, P. 2005, *ApJ*, 630, 495
- Khargharia, J., Froning, C. S., & Robinson, E. L. 2010, *The Astrophysical Journal*, 716, 1105
- Lattimer, J. M., & Prakash, M. 2016, *Phys. Rep.*, 621, 127
- Martini, P., Persson, S. E., Murphy, D. C., Birk, C., Shectman, S. A., Gunnels, S. M., & Koch, E. 2004, PANIC: a near-infrared camera for the Magellan telescopes
- Matsuoka, M. et al. 1980, *ApJ*, 240, L137
- Orosz, J. A., & Hauschildt, P. H. 2000, *A&A*, 364, 265
- Shahbaz, T., Naylor, T., & Charles, P. A. 1993, *MNRAS*, 265, 655
- Shahbaz, T., Watson, C. A., & Dhillon, V. S. 2014, *MNRAS*, 440, 504